ChemComm

Accepted Manuscript

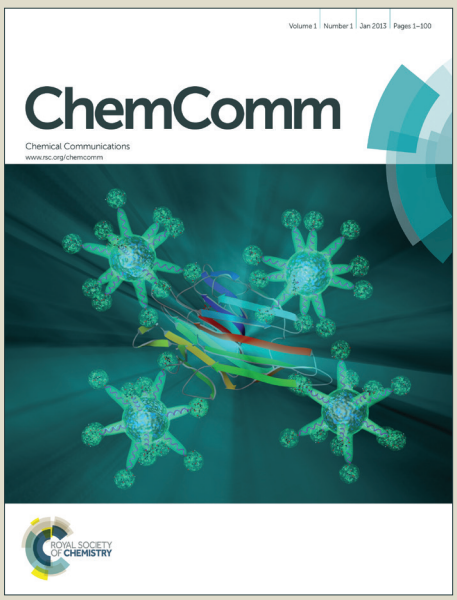

ROYAL SOCIETY OF CHEMISTRY

www.rsc.org/chemcomm

ChemComm

RSCPublishing

COMMUNICATION

Improved Electrocatalytic Activity for Ethanol Oxidation by Pd@N-doped Carbon from Biomass

Cite this: DOI: 10.1039/x0xx00000x

Haiyan Jin, Tianyi Xiong, Yi Li, Xuan Xu, Mingming Li and Yong Wang *

Received 00th January 2012,
Accepted 00th January 2012

DOI: 10.1039/x0xx00000x

www.rsc.org/

Pd@N-doped carbon (Pd@CN) exhibited four and two times higher peak current density toward ethanol electrooxidation than Pd@active carbon and Pd@non-nitrogen carbon. Controlled experimental results indicated that the incorporation of nitrogen into the carbon matrix improved the percentage of Pd^0 and increased the binding energy of Pd in Pd@CN, and accordingly enhancing the catalytic activity.

Accelerated depletion of fossil fuels, coupled with concerns over environmental pollution, poses great demands for renewable and clean energy sources.[1] From this standpoint of view, ethanol possesses distinct advantages over methanol, gas fuels etc. owing to its high energy density, low toxicity, easy storage and transportation, and large scale of production from biomass.[2] Accordingly, direct ethanol fuel cells (DEFCs) have been extensively studied in efforts as power sources for portable electronic devices and fuel cell vehicles. However, it is quite difficult to completely oxidize ethanol which involves breaking C-C bond and releasing 12 electrons.[3] Moreover, many adsorbed intermediates (mainly CO and -CHO) produced during the oxidation reaction poison the anode catalysts and in turn reduce the catalytic efficiency.[4] Therefore, it necessitates high activity and stability electrocatalysts to accelerate this reaction.

It's well known that Pd is a promising electrocatalyst for ethanol oxidation in basic media.[5] Great research efforts have been devoted to adding a second element such as Sn[6], Ni[7], Bi[8], Ag[9], Au[10], Pb[11] to Pd supported on carbon materials to optimize the electrocatalytic performance and stability of Pd toward ethanol oxidation in alkaline media because of the bimetallic synergistic effect. However, the influence of support materials on the valence state, size distribution, stability and dispersion of Pd which further affects its catalytic property and efficiency cannot be overlooked.[12]

Currently, nitrogen-doped carbon materials as supports have received particular attention to researchers due to their remarkable performance in various applications, such as hydrocarbon oxidation[13], hydrogenation of unsaturated bond[14], biomass refining[15], etc. Furthermore, the use of inexpensive, sustainable feedstocks to produce N-doped carbon materials conforms to the concept of green chemistry.[16] And the reasons may contribute to the fact that the incorporation of electron-rich nitrogen atoms modifies the surface structure of carbon materials, demonstrating improved π-binding ability, more defects and strengthened interaction between metal nanoparticles (NPs) and supports.[17]

Based on the above considerations, herein, N-doped mesoporous carbon material from D-glucosamine hydrochloride, a harmless and naturally available biomass, was utilized as a basic support to construct Pd catalysts (Pd@CN, the content of nitrogen in CN is about 7.0%) towards ethanol oxidation in alkaline media. Compared to Pd@HC (non-nitrogen hydrothermal carbon from glucose) and the commercially available Pd@AC, Pd@CN demonstrated superior catalytic performance for ethanol oxidation. The influences of pore structure and surface area of supports and valence state and morphology of metal palladium were investigated in detail towards ethanol oxidation. Physical and electrochemical datas indicated that the incorporation of nitrogen could enhance the percentage of Pd^0 and increase the binding energy of Pd in Pd@CN which produced superior catalytic activity.

To evaluate the catalytic properties of Pd@CN versus Pd@HC and Pd@AC catalysts toward ethanol oxidation, we performed the electrooxidation reaction of these catalysts in 1 M C_2H_5OH + 1 M KOH. The CVs at 50 mV/s (Fig. 1a) show that the specific peak current density of Pd@CN is almost two and four times higher than that of Pd@HC and Pd@AC when the current density is normalized to per unit mass of Pd. In addition, the onset potential of the forward scan direction of Pd@CN is remarkably lower than that of Pd@HC and Pd@AC, which is an evidence that Pd@CN overtakes Pd@HC and Pd@AC in the kinetics of ethanol oxidation reaction.[18]

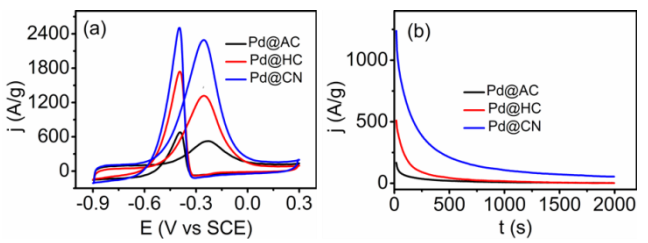

Fig. 1. (a) CVs of Pd@AC, Pd@HC, and Pd@CN in 1 M C_2H_5OH + 1 M KOH solution at 50 mV/s. (b) Chronoamperometric curves of three catalysts measured in the solution of 1 M KOH + 1 M C_2H_5OH at -0.35V.

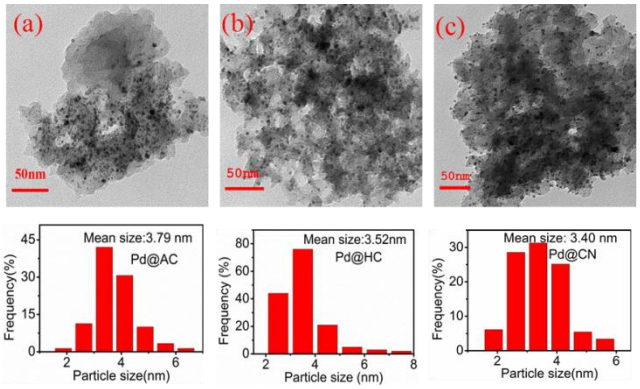

Fig. 2. TEM images and corresponding particle size distribution histograms for (a) Pd@AC, (b) Pd@HC, (c) Pd@CN.

To further confirm the high catalytic activity of Pd@CN, cyclic voltammetry tests of three catalysts were carried out in 1 M CH_3OH + 1 M KOH solution at a scan rate of 50 mV/s (Fig. S1, ESI†). It is evident that Pd@CN still shows higher activity towards methanol oxidation than Pd@HC and Pd@AC. The electrochemical stability of these catalysts for ethanol oxidation was then investigated by chronoamperometric experiments at a given potential of –0.35 V in 1.0 M KOH + 1.0 M C_2H_5OH solution (Fig. 1b). As shown that Pd@CN exhibits a slower current decay over time in comparison with Pd@HC and Pd@AC, proving a higher tolerance to carbonaceous species generated during ethanol oxidation.[19]

The above results demonstrate Pd@CN exhibits higher electrocatalytic activity and better durability than Pd@HC and Pd@AC. It has been proven that the dispersion and valence state of Pd and structure properties (BET surface area, pore structure) of supports can affect the activity of catalysts.[20] The following detailed discussions elaborated the decisive factors in perfecting the performance of Pd@CN towards ethanol oxidation.

As presented in Fig. 2, The Pd NPs are uniformly dispersed on supports. Size distribution histograms demonstrate the average particle sizes of Pd@AC, Pd@HC, and Pd@CN are 3.79, 3.52, and 3.40nm, respectively, suggesting similar size distributions. Moreover, the dispersions (D) of Pd in Pd@AC, Pd@HC, and Pd@CN, i.e., the fraction of exposed Pd in the catalyst are determined to be 0.26, 0.28, and 0.29, respectively (ESI†).[21] The similar particle size and dispersion of Pd in catalysts make it possible to eliminate the effect of metal particle size and dispersion on ethanol electrooxidation activity.[22] The XRD patterns of three catalysts (Fig. S2, ESI†) together with the TEM images indicate similar metal morphology structure[23], excluding the influence of metal crystal structure on ethanol oxidation in this case, which inspires us to further discuss other factors influencing catalyst performance.

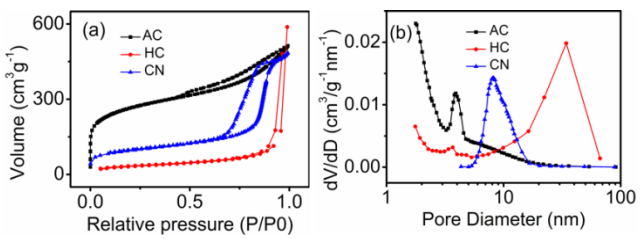

Fig. 3. (a) N_2 adsorption/desorption isotherms and (b) corresponding Barrett-Joyner-Halenda (BJH) pore-size distribution curve determined from the desorption branch of the isotherm of AC, HC, CN.

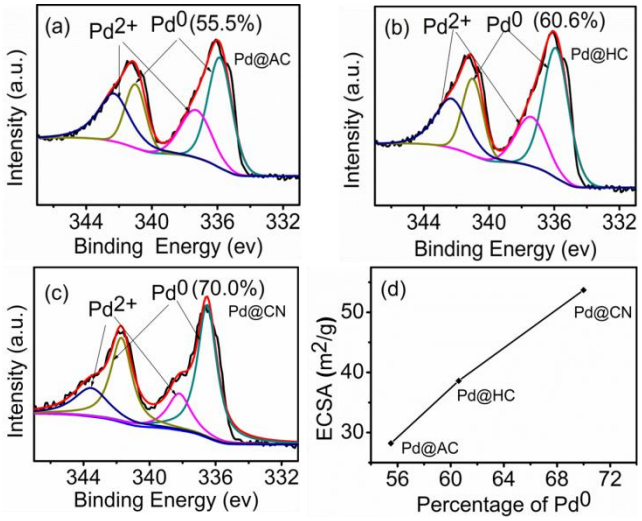

Fig. 4. The Pd_{3d} X-ray photoelectron spectroscopies of (a) Pd@AC, (b) Pd@HC, and (c) Pd@CN and (d) The correlation pattern of ECSA and percentage of Pd^0 of Pd@AC, Pd@HC, and Pd@CN.

The pore structure and surface area of AC, HC, and CN were then investigated by N_2 adsorption-desorption isotherms. As shown in Fig. 3a and b, AC mainly consists of micropores and mesopores, and accumulated pores dominate HC with wide pore distribution. Meanwhile, CN exhibits a IV-type isotherm with a distinct hysteretic loop, indicating the mesoporous nature. Though the BET surface area of CN (324 m^2/g) and HC (115 m^2/g) are smaller than AC (899 m^2/g) (Table S1, ESI†), their electrocatalytic performances as supports are still superior to AC, indicating the larger surface area doesn't always produce better catalytic activity. The larger pore size distribution of CN (8nm) and HC (34nm) could yield easier mass transportation and consequently better performance towards ethanol oxidation than AC with pore diameter of 4nm (Table S1, ESI†).[24] Though the pore volume of CN is smaller than HC, it still presents better activity. The above results illustrate that proper BET surface area, pore size and pore volume are necessary to improve ethanol electrooxidation activity of catalysts.

The Pd_{3d} X-ray photoelectron spectroscopies (XPS) of three catalysts are shown in Fig. 4. The survey XPS spectrum of Pd@CN confirms the incorporation of nitrogen into carbon materials (Fig. S3, ESI†). The Pd_{3d} signal of Pd@HC catalyst is fitted to two pairs of doubles: $Pd_{3d3/2}$ (337.4 eV), $Pd_{3d5/2}$ (335.9 eV) and $Pd_{3d3/2}$ (342.3 eV) $Pd_{3d5/2}$ (341 eV), which can be ascribed to Pd^0 and Pd^{2+} species, respectively.[25] However, the binding energy of Pd^0 (341.7 eV, 336.5 eV) and Pd^{2+} (338.2 eV, 343.6 eV) in Pd@CN positively shift, respectively (Table S2, ESI†). Meanwhile, the binding energy of pyridic-N, pyrrolic-N and quaternary-N of Pd@CN negatively shift compared with that of CN (Fig. S4 and Table S3, ESI†), implying a transfer of electron density from N to Pd.[26] Therefore, the incorporation of nitrogen is beneficial to the reduction of Pd^{2+} to Pd^0 due to the electron donation effects of nitrogen, which provides more active sites and accordingly will improve the catalytic activity of Pd@CN.[14a, 27] This can also be confirmed by the fact that Pd@CN possesses the most percentage of Pd^0 (70.0%) among three catalysts due to the N-doping effect (Table S2, ESI†). Moreover, the positive shift of binding energy of Pd can be attributed to the introduction of nitrogen, which reflects the downshift of d-band center of Pd atom in Pd@CN and consequently results in the decrease in the interaction strength of various adsorbents to Pd surface.[25, 28]

To further illustrate the nitrogen-doping effect on ethanol electrooxidation, we performed CVs and CO stripping experiments

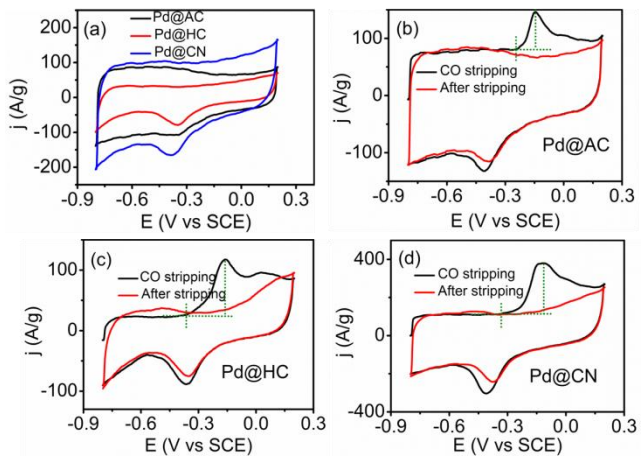

Fig. 5. (a) CVs of Pd@AC, Pd@HC, and Pd@CN in 1 M KOH solution. Scan rate: 50mV s^{-1}. CO stripping measurements of (b) Pd@AC, (c) Pd@HC, and (d) Pd@CN performed in 1 M KOH solution at 50mV/s.

on three catalysts in 1.0 M KOH solution at 50 mV/s (Fig. 5). The calculated electrochemically surface area (ECSA) of Pd@CN catalyst is 1.9 and 1.4 times greater than Pd@AC and Pd@HC (table S1, ESI†).[29] The above results prove that a higher proportion of Pd is electrochemically available in Pd@CN than Pd@HC and Pd@AC. As shown in Fig. 4d, the ECSA presents some degree of linear relationship with the percentage of Pd^0, again revealing the effect of N-doping on the improved percentage of Pd^0 in CN. We also compared the surface area normalized activity (A/m^2) based the electrochemical surface area of Pd in Fig. S5 (ESI†). Results also show that Pd@CN catalyst still offers much higher electrocatalytic activity than Pd@HC and Pd@AC. The results of CO stripping experiments on three catalysts are shown in Fig. 5b, c and d. An obviously larger CO oxidation peak than that on Pd@HC and Pd@AC catalyst in the initial forward scan is observed on Pd@CN catalyst owning to a larger ECSA of Pd. In addition, the initial potential of CO oxidation on Pd@CN (-0.35 V) is slightly more negative than that of on Pd@HC (-0.34 V), but significantly lower than Pd@AC (-0.25 V) in first forward scan.[30] These results can be attributed to the introduction of N which lower the adsorption strength of CO and facilitate removal of CO on the surface of catalyst. The disappearance of CO oxidation peaks after stripping and reappearance of hydrogen peaks at negative potentials indicate that both catalysts are free of dissolved CO.

Conclusions

In conclusion, we applied a biomass-derived nitrogen-doped carbon material as a desired support of Pd to direct ethanol fuel cells. Compared to Pd@AC and Pd@HC, Pd@CN exhibited four and two times higher peak current density toward ethanol oxidation, respectively. Research results illustrated that proper BET surface area, pore size, and pore volume were beneficial to improving the ethanol electrooxidation activity of catalysts. XPS experiments further proved that the introduction of nitrogen into carbon matrix improved the percentage of Pd^0 and increased the binding energy of Pd in Pd@CN, and accordingly enhancing the catalytic activity, durability and CO tolerance of catalyst. Thus, nitrogen-doped carbon materials as high-performance catalyst supports have great promising application in direct ethanol fuel cells.

Financial support from the National Natural Science Foundation of China (21376208 & U1162124), the Zhejiang Provincial Natural Science Foundation for Distinguished Young Scholars of China (LR13B030001), the Specialized Research Fund for the Doctoral Program of Higher Education (J20130060), the Fundamental Research Funds for the Central Universities, the Program for Zhejiang Leading Team of S&T Innovation, the Partner Group Program of the Zhejiang University and the Max-Planck Society are greatly appreciated.

Notes and references

*Carbon Nano Materials Group, ZJU-NHU United R&D Center, Center for Chemistry of High-Performance and Novel Materials, Key Lab of Applied Chemistry of Zhejiang Province, Department of Chemistry, Zhejiang University, Hangzhou 310028, P. R. China. Fax: (+86)-571-8795-1895; Tel: (+86)-571-8827-3551; E-mail: chemwy@zju.edu.cn.

†Electronic Supplementary Information (ESI) available: Experimental details, Figure S1-S5 and Table S1-S3. See DOI: 10.1039/b000000x/

1 M. Li, D. A. Cullen, K. Sasaki, N. S. Marinkovic, K. More and R. R. Adzic, *J. Am. Chem. Soc.*, 2013, **135**, 132.

2 (a) L. Ren, K. S. Hui and K. N. Hui, *J. Mater. Chem. A*, 2013, **1**, 5689; (b) S. Song and P. Tsiakaras, *Appl. Catal., B*, 2006, **63**, 187.

3 A. Kowal, M. Li, M. Shao, K. Sasaki, M. B. Vukmirovic, J. Zhang, N. S. Marinkovic, P. Liu, A. I. Frenkel and R. R. Adzic, *Nat. Mater.*, 2009, **8**, 325.

4 J. Datta, A. Dutta and S. Mukherjee, *J. Phys. Chem. C*, 2011, **115**, 15324.

5 (a) J. W. Hong, Y. W. Lee, M. Kim, S. W. Kang and S. W. Han, *Chem. Commun.*, 2011, **47**, 2553; (b) C. Zhu, S. Guo and S. Dong, *Adv. Mater.*, 2012, **24**, 2326.

6 L. X. Ding, A. L. Wang, Y. N. Ou, Q. Li, R. Guo, W. X. Zhao, Y. X. Tong and G. R. Li, *Sci. Rep-Uk*, 2013, **3**, 1181.

7 Y. Wang, F.-F. Shi, Y.-Y. Yang and W.-B. Cai, *J. Power Sources*, 2013, **243**, 369.

8 A. Zalineeva, S. Baranton and C. Coutanceau, *Electrochem. Commun.*, 2013, **34**, 335.

9 (a) S. T. Nguyen, Y. Yang and X. Wang, *Appl. Catal.*, B, 2012, **113-114**, 261; (b) S. T. Nguyen, H. M. Law, H. T. Nguyen, N. Kristian, S. Wang, S. H. Chan and X. Wang, *Appl. Catal., B*, 2009, **91**, 507.

10 W. J. Wang, J. Zhang, S. C. Yang, B. J. Ding and X. P. Song, *Chemsuschem*, 2013, **6**, 1945.

11 Y. Wang, T. S. Nguyen, X. Liu and X. Wang, *J. Power Sources*, 2010, **195**, 2619.

12 (a) S. Song, S. Yin, Z. Li, P. K. Shen, R. Fu and D. Wu, *J. Power Sources*, 2010, **195**, 1946; (b) J. Yang, C. Tian, L. Wang and H. Fu, *J. Mater. Chem. A*, 2011, **21**, 3384; (c) X. S. Zhao, W. Z. Li, L. H. Jiang, W. J. Zhou, Q. Xin, B. L. Yi and G. Q. Sun, *Carbon*, 2004, **42**, 3263.

13 M. Soorholtz, R. J. White, T. Zimmermann, M.-M. Titirici, M. Antonietti, R. Palkovits and F. Schueth, *Chem. Commun.*, 2013, **49**, 240.

14 (a) Y. Wang, J. Yao, H. Li, D. Su and M. Antonietti, *J. Am. Chem. Soc.*, 2011, **133**, 2362; (b) X. Xu, M. Tang, M. Li, H. Li and Y. Wang, *ACS Catal.*, 2014, **4**, 3132.

15 (a) X. Xu, Y. Li, Y. Gong, P. Zhang, H. Li and Y. Wang, *J. Am. Chem. Soc.*, 2012, **134**, 16987; (b) M. Li, X. Xu, Y. Gong, Z. Wei, Z. Hou, H. Li and Y. Wang, *Green Chem.*, 2014, **16**, 4371.

16 R. J. White, N. Yoshizawa, M. Antonietti and M.-M. Titirici, *Green Chem.*, 2011, **13**, 2428.

17 (a) P. Zhang, Y. Gong, H. Li, Z. Chen and Y. Wang, *Nat. Commun.*, 2013, **4**, 1593; (b) P. Chen, L. M. Chew, A. Kostka, M. Muhler and W. Xia, *Catal. Sci. Technol*, 2013, **3**, 1964.
18 Y. X. Chen, A. Lavacchi, S. P. Chen, F. di Benedetto, M. Bevilacqua, C. Bianchini, P. Fornasiero, M. Innocenti, M. Marelli, W. Oberhauser, S. G. Sun and F. Vizza, *Angew. Chem. Int. Ed.*, 2012, **51**, 8500.
19 J. F. Gomes, K. Bergamaski, M. F. S. Pinto and P. B. Miranda, *J. Catal.*, 2013, **302**, 67.
20 (a) V. Ravat, I. Nongwe, R. Meijboom, G. Bepete and N. J. Coville, *J. Catal.*, 2013, **305**, 36; (b) L. Calvillo, V. Celorrio, R. Moliner, A. B. Garcia, I. Cam én and M. J. Lazaro, *Electrochim. Acta*, 2013, **102**, 19.
21 Y. Li, X. Xu, P. Zhang, Y. Gong, H. Li and Y. Wang, *Rsc. Adv.*, 2013, **3**, 10973.
22 W. Zhou and J. Y. Lee, *J. Phys. Chem. C*, 2008, **112**, 3789.
23 N. Tian, Z.-Y. Zhou, N.-F. Yu, L.-Y. Wang and S.-G. Sun, *J. Am. Chem. Soc., 2010, 132, 7580.*
24 Z. Yan, Z. Hu, C. Chen, H. Meng, P. K. Shen, H. Ji and Y. Meng, *J. Power Sources*, 2010, **195**, 7146.
25 K. Wu, X. Mao, Y. Liang, Y. Chen, Y. Tang, Y. Zhou, J. Lin, C. Ma and T. Lu, *J. Power Sources*, 2012, **219**, 258.
26 (a) P. Luksirikul, K. Tedsree, M. G. Moloney, M. L. H. Green and S. C. E. Tsang, *Angew. Chem. Int. Ed.*, 2012, **51**, 6998; (b) B. Xiong, Y. Zhou, Y. Zhao, J. Wang, X. Chen, R. O'Hayre and Z. Shao, *Carbon*, 2013, **52**, 181.
27 X. Chen, G. Wu, J. Chen, X. Chen, Z. Xie and X. Wang, *J. Am. Chem. Soc.*, 2011, **133**, 3693.
28 M. Zhao, K. Abe, S.-i. Yamaura, Y. Yamamoto and N. Asao, *Chem. Mater.*, 2014, **26**, 1056.
29 W. Pan, X. Zhang, H. Ma and J. Zhang, *J. Phys. Chem. C*, 2008, **112**, 2456.
30 A. L. Wang, H. Xu, J. X. Feng, L. X. Ding, Y. X. Tong and G. R. Li, *J. Am. Chem. Soc.*, 2013, **135**, 10703.

